Dynamic Pinhole SPECT Imaging and Compartmental Modeling of Fatty Acid Metabolism in the Rat Heart

Bryan W. Reutter, *Senior Member, IEEE,* Rostyslav Boutchko, *Member, IEEE,*
Ronald H. Huesman, *Fellow, IEEE,* Stephen M. Hanrahan, Kathleen M. Brennan, Anne C. Sauve,
and Grant T. Gullberg, *Fellow, IEEE*

***Abstract*—The goal of this work is to quantitatively compare fatty acid metabolism in the hearts of normal and spontaneously hypertensive rats (SHR) as a function of age, and thereby track physiological changes associated with the onset and progression of heart failure in the SHR model. We imposed a more-stringent negativity penalty for fully 4-D multiresolution B-spline SPECT image reconstruction, and applied this method to obtain weighted least-squares estimates of time-activity curves directly from projections for dynamic pinhole SPECT studies of ^{123}I-labeled BMIPP fatty acid analog in the myocardium of both a normal rat and an SHR. Dynamic projection data were acquired for 60 min in 1-sec time frames with an angular step of 4 degrees per frame on a dual-head GE Millennium VG Hawkeye SPECT/CT scanner equipped with custom pinhole collimators. The time-varying spatial distribution of ^{123}I-BMIPP was modeled with use of 4-D multiresolution B-splines that were piecewise constant in space and piecewise quadratic in time. The 4-D splines were organized on a 3-D spatial grid that provided sampling of 3.2 mm near the heart and 6.4 mm away from the heart. Temporal sampling intervals were 0–2.4, 2.4–9.4, 9.4–30, and 30–90 sec during the first gantry rotation. The use of nonuniform time sampling with B-splines that varied quadratically in time yielded smooth time-activity curves that captured the relatively fast rise and fall of ^{123}I-BMIPP in the left ventricular blood pool, as well as the uptake and trapping of the radiotracer in the left ventricular myocardium. Compartmental modeling was then applied to the time-activity curves. This yielded quantitative metabolic rate estimates (K_i) of 0.60 min^{-1} and 0.22 min^{-1} in the normal and SHR hearts, respectively. The slower rate of fatty acid metabolism in the SHR is what one expects as the SHR heart switches to a reliance on glycolysis as the primary pathway for energy production during the development of heart failure. This fully 4-D image reconstruction method can also be applied to dynamic PET.**

I. Introduction

THE goal of this work is to quantitatively compare fatty acid metabolism in the hearts of Wistar-Kyoto (WKY) normal rats and spontaneously hypertensive rats (SHR) as a function of age, and thereby track physiological changes associated with the onset and progression of heart failure in the SHR model.

The fatty acid analog, ^{123}I-labeled BMIPP, was used in longitudinal metabolic imaging studies performed every seven months. Slow rotation of the SPECT camera necessitated modeling the radiotracer time variation in the tomographic image reconstruction algorithm, which yielded time-activity curve estimates for the blood and myocardium directly from dynamic projection data.

This work builds on our previous work in fully 4-D multiresolution SPECT image reconstruction [1], [2]. In the work presented here, a more-stringent negativity penalty is imposed to obtain less-noisy, weighted least-squares estimates of time-activity curves directly from projections for dynamic pinhole SPECT studies of ^{123}I-BMIPP in the myocardium of both a WKY normal rat and an SHR. Compartmental modeling is then applied to the time-activity curves to obtain quantitative estimates of the metabolic rate of ^{123}I-BMIPP in the myocardium. Results are presented for metabolic imaging studies performed in rats aged 21 months, when the SHR was nearing end-stage congestive heart failure.

This fully 4-D image reconstruction method can also be applied to dynamic PET.

II. Methods

A. Pinhole SPECT Data Acquisition and System Modeling

With use of methods described in [3], dynamic cardiac pinhole SPECT projection data and pinhole geometric calibration data were acquired on a dual-head GE Millennium VG Hawkeye SPECT/CT scanner equipped with custom pinhole

Fig. 1. Clinical dual-head SPECT/CT scanner with custom pinhole collimators used for quantitative dynamic imaging of fatty acid metabolism in the rat heart.

This work was supported by the National Institutes of Health of the U. S. Department of Health and Human Services under grants R01-EB00121, R01-EB007219, and R01-HL71253; and by the Director, Office of Science, Office of Biological and Environmental Research of the U. S. Department of Energy under contract DE-AC02-05CH11231.

B. W. Reutter, R. Boutchko, R. H. Huesman, S. M. Hanrahan, K. M. Brennan, A. C. Sauve, and G. T. Gullberg are with the Department of Imaging Technology, Lawrence Berkeley National Laboratory, One Cyclotron Road, Berkeley, CA 94720, USA (e-mail: bwreutter@lbl.gov).

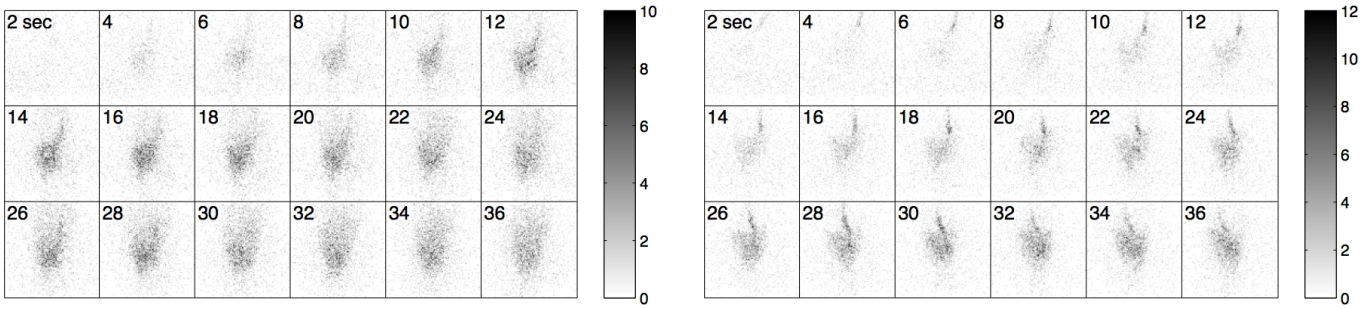

(a) WKY normal (b) SHR

Fig. 2. Dynamic cardiac ^{123}I-BMIPP pinhole SPECT projection data acquired by one detector head during the interval 2–36 sec for (a) the WKY normal rat and (b) the SHR. These early time frames show the arrival of the injected bolus at the heart, followed by initial uptake in the myocardium. The maximum numbers of counts in a detector bin are 10 and 12 for the WKY normal rat and SHR, respectively.

collimators (Fig. 1). For each study, an injection of about 4 mCi of ^{123}I-BMIPP was performed shortly after the dynamic data acquisition began. Data were acquired for 60 min in 1-sec time frames with an angular step of 4 degrees per frame (Fig. 2). Collimator response was modeled via ray tracing and excluded the effects of collimator penetration. The system model also excluded the effects of attenuation and scatter; however, we are currently studying these effects via Monte Carlo simulation in a separate investigation [4], [5].

B. Fully 3-D Late Static Image Reconstruction

To determine spatial locations for the left ventricular blood pool and myocardial tissue, late data acquired 1.5–60 min after injection were summed and a static image was reconstructed with use of a computationally efficient fully 3-D weighted least-squares method based on that described in [1]. The late static spatial distribution of ^{123}I-BMIPP was modeled with use of 3-D multiresolution spatial B-splines that were piecewise constant. The 3-D spatial splines were organized on a 20×20×20 3-D grid that provided uniform sampling of 3.2 mm in each dimension. Inside the volume containing the heart, a 6×6×6 neighborhood of these lower-resolution splines was replaced by a 12×12×12 neighborhood of higher-resolution splines that provided uniform sampling of 1.6 mm.

C. Fully 4-D Early Dynamic Image Reconstruction

To quantify fatty acid metabolism in the rat heart, early data acquired 0–1.5 min after injection were not summed and a dynamic image was reconstructed with use of a computationally efficient fully 4-D weighted least-squares method based on that described in [2]. The time-varying spatial distribution of ^{123}I-BMIPP was modeled with use of 4-D multiresolution B-splines that were piecewise constant in space and piecewise quadratic in time. The 4-D splines were spatially organized on a 10×10×10 3-D grid that provided uniform sampling of 6.4 mm in each dimension. Inside the volume containing the heart, a 3×3×3 neighborhood of these lower-resolution splines was replaced by a 6×6×6 neighborhood of higher-resolution splines that provided uniform sampling of 3.2 mm. The 4-D splines were temporally organized on a 1-D grid that provided nonuniform sampling intervals of 0–2.4, 2.4–9.4, 9.4–30, and 30–90 sec during the first gantry rotation (Fig. 3).

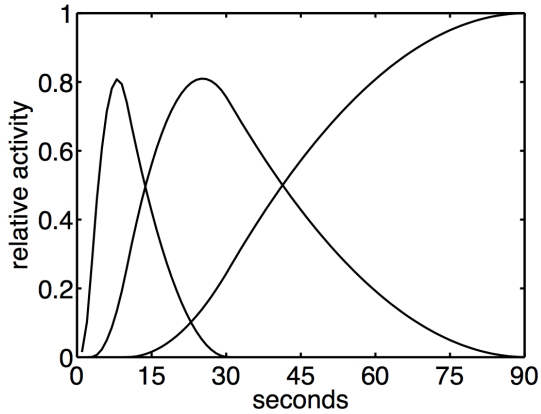

Fig. 3. Piecewise quadratic temporal B-spline basis functions used to reconstruct dynamic data from the first gantry rotation.

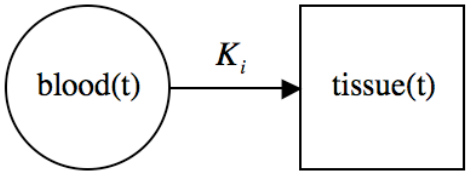

Fig. 4. One-tissue-compartment model used for quantifying fatty acid metabolism during the first 1.5 min after injection of ^{123}I-BMIPP.

D. Negativity Penalty

When reconstructing both the 3-D static late image and the 4-D dynamic early image, B-spline coefficients that tended to have negative values were identified with use of an iterative algorithm that converged quickly [1]. These spline coefficients were then constrained to stay near zero with use of a quadratic penalty that penalized nonzero contributions to the projection data model. As a result of the penalty, the constrained coefficients ultimately had a mean value of approximately zero and image noise was reduced significantly. The constrained coefficients were also negatively correlated, as one would expect for a tomographic image reconstructed from projection data measurements that are essentially line integrals.

In the work that we present here, the negativity penalty is

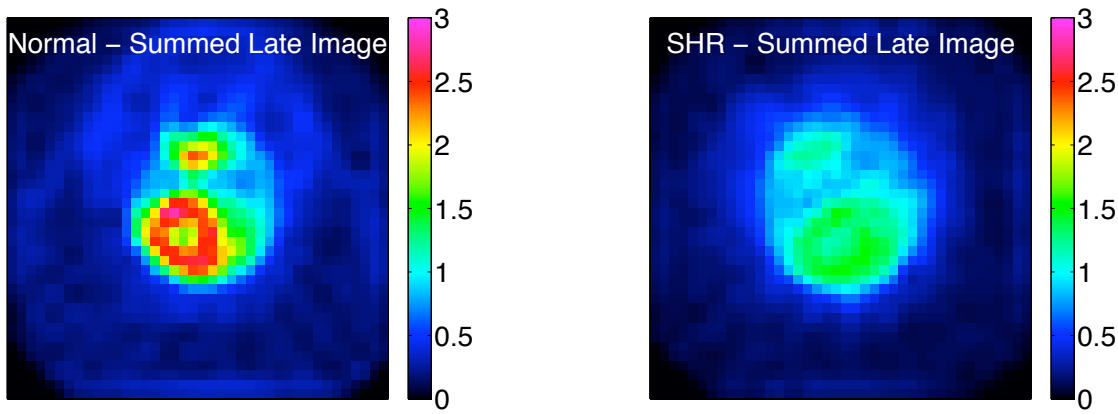

(a) WKY normal

(b) SHR

Fig. 5. More trapping of ^{123}I-BMIPP is evident in late 3-D static images of (a) the WKY normal heart, compared to (b) the SHR heart.

proportional to

$$\sum_{i=1}^{I}\sum_{m=1}^{M}\left(F_{im}N_m a_m\right)^2, \tag{1}$$

where F_{im} is the (i,m)-th element of an $I \times M$ system matrix; I is the number of dynamic projection data bins; M is the number of B-spline basis functions that span the space and time to be reconstructed; a_m is the m-th element of an M-element column vector of spline coefficients; and N_m is an indicator function that is one if the penalty is to be applied to the m-th coefficient, or zero otherwise.

For the resulting negatively correlated, zero-mean, constrained coefficients, Eq. (1) imposes a penalty that is greater than the penalty imposed by the quadratic form that we used in [1]:

$$\sum_{i=1}^{I}\left(\sum_{m=1}^{M}F_{im}N_m a_m\right)^2. \tag{2}$$

In particular, the more-stringent penalty imposed by Eq. (1) is effective in reducing the magnitude of negative coefficients associated with the earliest temporal B-spline basis function that spans the time period of 0–30 sec.

E. Compartmental Modeling of Fatty Acid Metabolism

Left ventricular blood pool and myocardial tissue locations were identified in the late 3-D static image, and time-activity curves were obtained by sampling the early 4-D dynamic image at these locations. The program RFIT [6]–[8] was then used to fit a one-tissue-compartment model (Fig. 4) to the time-activity curves to obtain a quantitative estimate of the metabolic rate of ^{123}I-BMIPP in the rat myocardium. Early myocardial tissue uptake was modeled with a single, irreversible compartment:

$$\text{tissue}(t) = K_i \cdot \int_0^t \text{blood}(\tau)d\tau, \tag{3}$$

where K_i is the metabolic rate of ^{123}I-BMIPP. Myocardial tissue voxels were modeled as mixture of blood input and tissue uptake:

$$\text{voxel}(t) = \left[f_v \cdot \text{blood}(t)\right] + \left[K_i \cdot \int_0^t \text{blood}(\tau)d\tau\right], \tag{4}$$

where f_v is the fraction of vasculature in the tissue and also incorporates the effect of spillover from the blood pool to the tissue.

III. Results

In the late 3-D static images (Fig. 5), more trapping of ^{123}I-BMIPP is evident in the WKY normal heart, compared to the SHR heart.

For the early 4-D dynamic images, the use of nonuniform time sampling with splines that varied quadratically in time yielded smooth time-activity curves (Fig. 6) that captured the relatively fast rise and fall of ^{123}I-BMIPP in the left ventricular blood pool, as well as the uptake and initial trapping of the radiotracer in the left ventricular myocardium.

From these time-activity curves, compartmental modeling yielded estimates of $K_i = 0.60$ min^{-1} and $K_i = 0.22$ min^{-1} for the metabolic rates of ^{123}I-BMIPP in the WKY normal rat and the SHR, respectively. The slower rate of fatty acid metabolism in the SHR is what one expects as the SHR heart switches to a reliance on glycolysis as the primary pathway for energy production during the development of heart failure.

IV. Discussion

This analysis method enables quantitative dynamic imaging of fatty acid metabolism in the rat heart, even with slow camera rotation. To the best of our knowledge, no other group has successfully developed a method to reconstruct the blood input function from small animal dynamic pinhole SPECT data acquired with slow camera rotation.

Future work includes addressing computational issues associated with reconstructing a dynamic image from the entire 60 min of projection data. It is anticipated that an additional washout parameter will be needed in the one-tissue-compartment model to account for washout of ^{123}I-BMIPP from the myocardium over this longer time scale.

This fully 4-D image reconstruction method can also be applied to dynamic PET.

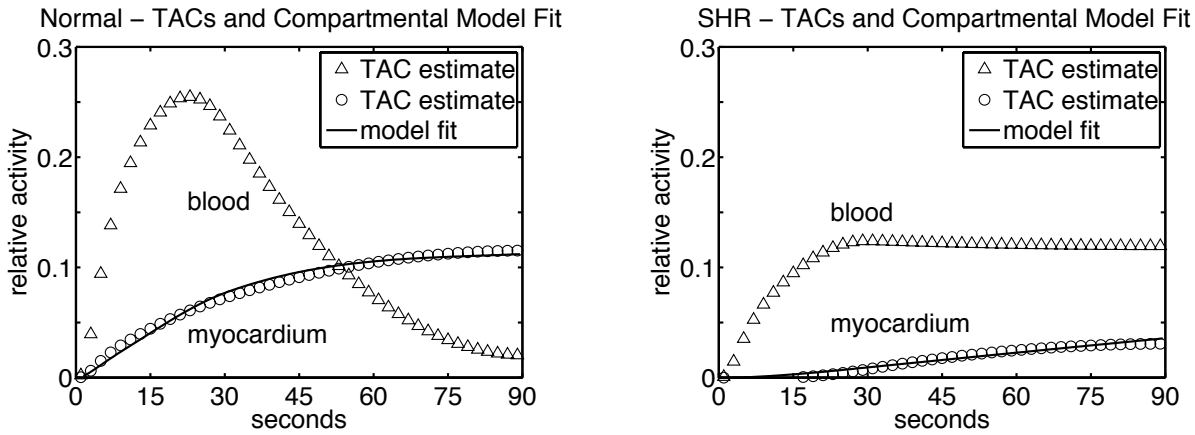

(a) WKY normal: $K_i = 0.60$ min^{-1}

(b) SHR: $K_i = 0.22$ min^{-1}

Fig. 6. Time-activity curves for (a) the WKY normal rat and (b) the SHR capture quantitative differences between their blood inputs and myocardial uptakes (triangles and circles, respectively). Compartment models provide good fits (solid lines) to the time-activity curves for the myocardium and provide quantitative estimates of the metabolic rate of ^{123}I-BMIPP (K_i).

ACKNOWLEDGMENT

This work was supported by the National Institutes of Health of the U. S. Department of Health and Human Services under grants R01-EB00121, R01-EB007219, and R01-HL71253; and by the Director, Office of Science, Office of Biological and Environmental Research of the U. S. Department of Energy under contract DE-AC02-05CH11231.

This document was prepared as an account of work sponsored by the United States Government. While this document is believed to contain correct information, neither the United States Government nor any agency thereof, nor The Regents of the University of California, nor any of their employees, makes any warranty, express or implied, or assumes any legal responsibility for the accuracy, completeness, or usefulness of any information, apparatus, product, or process disclosed, or represents that its use would not infringe privately owned rights. Reference herein to any specific commercial product, process, or service by its trade name, trademark, manufacturer, or otherwise, does not necessarily constitute or imply its endorsement, recommendation, or favoring by the United States Government or any agency thereof, or The Regents of the University of California. The views and opinions of authors expressed herein do not necessarily state or reflect those of the United States Government or any agency thereof or The Regents of the University of California.

REFERENCES

[1] B. W. Reutter, G. T. Gullberg, R. Boutchko, K. Balakrishnan, E. H. Botvinick, and R. H. Huesman, "Regularized least-squares SPECT image reconstruction using multiresolution spatial B-splines and a negativity penalty," in *Proceedings of the 9th International Conference on Fully Three-Dimensional Image Reconstruction in Radiology and Nuclear Medicine*, M. Kachelrieß and F. Beekman, Eds., 2007, pp. 305–308.

[2] ——, "Fully 4-D dynamic cardiac SPECT image reconstruction using spatiotemporal B-spline voxelization," in *2007 IEEE Nuclear Science Symposium and Medical Imaging Conference Record*, B. Yu, Ed., 2007, pp. 4217–4221.

[3] J. Hu, A. Sitek, B. W. Reutter, R. H. Huesman, and G. T. Gullberg, "A new approach of dynamic pinhole SPECT imaging for evaluation of sympathetic nervous system function in animal models of cardiac hypertrophy," in *2005 IEEE Nuclear Science Symposium and Medical Imaging Conference Record*, B. Yu, Ed., 2005, pp. 2542–2546.

[4] A. Sauve, W. Choong, R. Boutchko, B. W. Reutter, A. Hwang, E. W. Izaguirre, B. H. Hasegawa, and G. T. Gullberg, "Quantitative imaging of cardiovascular function with pinhole SPECT in mice and rats — effects of attenuation and scatter," *J Nucl Med*, vol. 48, no. 5 suppl, pp. 424P–425P, 2007 (abstract).

[5] A. C. Sauve, B. W. Reutter, R. Boutchko, W.-S. Choong, and G. T. Gullberg, "Multi-slice SPECT attenuation and scatter correction using Monte Carlo simulated system matrices," in *2008 IEEE Nuclear Science Symposium and Medical Imaging Conference Record*, P. Sellin, Ed., 2008 (in press).

[6] R. H. Huesman, B. L. Knittel, B. M. Mazoyer, P. G. Coxson, E. M. Salmeron, G. J. Klein, B. W. Reutter, and T. F. Budinger, "Notes on RFIT: A program for fitting compartmental models to region-of-interest dynamic emission tomography data," Lawrence Berkeley National Laboratory, Tech. Rep. LBL-37621, 1995.

[7] B. W. Reutter, G. T. Gullberg, and R. H. Huesman, "Direct least-squares estimation of spatiotemporal distributions from dynamic SPECT projections using a spatial segmentation and temporal B-splines," *IEEE Trans Med Imag*, vol. 19, no. 5, pp. 434–450, 2000.

[8] ——, "Effects of temporal modelling on the statistical uncertainty of spatiotemporal distributions estimated directly from dynamic SPECT projections," *Phys Med Biol*, vol. 47, no. 15, pp. 2673–2683, 2002.